Environ Monit Assess (2015) 187: 508
DOI 10.1007/s10661-015-4701-5

Mesoscale process-induced variation of the West India Coastal Current during the winter monsoon

V. K. Jineesh · K. R. Muraleedharan · K. Lix John · C. Revichandran · P. V. Hareesh Kumar · K. R. Naveen Kumar

Received: 5 May 2014 / Accepted: 18 June 2015 / Published online: 18 July 2015

Abstract This manuscript presents the analysis of current meter records at Kollam and Kannur along the 20-m isobaths during November–December 2005. Currents in the coastal waters are strongly influenced by winds (both local and remote forcing), tides, propagation of coastal Kelvin and Rossby waves, etc. We hypothesize that the mesoscale (spatial scales of 10–500 km and temporal scale of 10–100 days) features in ocean are also competent to alter the characteristics of coastal currents to a large extent. Analysis of sea level anomaly from the merged altimeter data reveals the existence of a large anticyclonic eddy in the southeastern Arabian Sea during the winter monsoon. The eddy moves westward with an average speed of ~15 km day^{-1} corresponding to an increase in sea level amplitude up to 28 cm. Off southwest India, the poleward flow is along the western flank of this anticyclonic eddy and the geostrophic current completes the circulation around the eddy. The eastward component of the geostrophic current at the northern edge of the eddy is bifurcated at ~9° N: one flowing towards north and the other towards south. Current meter records at station Kollam revealed a dominant southward current due to the bifurcated southward component. The bifurcated northward component coalesced with the poleward flow along the western flank of the anticyclonic eddy. At Kannur, a poleward flow along the coast is responsible for a predominant northward trend in the observed current pattern during the initial phase of observation. A reversal in the current direction is caused by the southward-flowing geostrophic current along the eastern flank of the subsequent anticyclonic eddy centered at 73.5° E and 13° N. The stations were located at the eastern periphery of these anticyclonic eddies, where the mesoscale features overwhelm the seasonal characteristics of the West India Coastal Current (WICC).

Keywords Coastal currents · Mesoscale eddies · Geostrophy · Winter monsoon · Eastern Arabian Sea

V. K. Jineesh (✉) · K. R. Muraleedharan · K. Lix John · C. Revichandran · K. R. Naveen Kumar
CSIR-National Institute of Oceanography, Regional Centre, Kochi, India
e-mail: jineeshvk@gmail.com

P. V. Hareesh Kumar
Naval Physical and Oceanographic Laboratory, Kochi, India

Introduction

The north Indian basin is essentially a tropical basin and has long been a region of interest due to the semi-annual reversal of the monsoon wind system. This introduces two seasons: summer monsoon from June to September and winter monsoon from November to February. The wind blows from southwest during the summer monsoon and from northeast during the winter monsoon. The prevailing winds during these seasons determine the circulation in this region and also the seasonality in surface currents. It is well known that variability in the winds over the basin with periods ranging from days to weeks can trigger the coastal currents with similar periods. The along-shore component of the local wind

stress has been identified as one of the principal forcing function for the along-shore coastal currents. The currents along the west coast of India called the West India Coastal Current (WICC) flows poleward carrying warmer and relatively fresh water from the Bay of Bengal during the winter monsoon and changes its direction towards the equator during the summer monsoon (Shetye et al. 1990; Shetye et al. 1991; Stramma et al. 1996; Shankar and Shetye 1997; Shetye and Gouveia 1998). Johannessen et al. (1981) pointed out that the coastal flow along the west coast reverses from a narrow, shallow, southward current to a wide, deep, northward flow having a larger mass transport against the prevailing winds during the winter monsoon. This property lends strong support for the importance of remote forcing. A number of studies have emphasized the importance of local and remote forcing for the circulation in the Arabian Sea (Bruce et al. 1994; Shankar and Shetye 1997; Bruce et al. 1998; Shenoi et al. 2004). Shetye et al. (2008) studied the contribution of both local and remote wind forcing for a month during March–April 2003 off Goa in the near-coast regime of the WICC. By using field measurements (current, sea level, and wind), they showed that the current was driven by local winds only at periods less than 10 days, with remote forcing contributing at longer periods. Recently, Amol et al. (2012) presented the evidence for poleward propagation of coastal-trapped waves on the shelf off the west coast of India from acoustic Doppler current profiler measurements. The currents in the north Indian basin are primarily due to free and forced tropical Rossby waves, equatorial Kelvin waves, and coastal Kelvin/shelf waves, triggered by the monsoonal winds (Shetye 1998). The equatorially and coastally trapped Kelvin waves in the North Indian Ocean play an important role in determining the nature of circulation in the coastal as well as in the open ocean (McCreary et al. 1993; Shankar et al. 2002).

The ocean circulation is indeed dominated by mesoscale variability, due to ocean eddies or isolated vortices, meandering currents or fronts, squirts, and filaments. Eddies which are between about 10 and 500 km in diameter and persist for periods of days to months are known as mesoscale eddies. These eddies are characterized by currents which flow in a roughly circular motion around the center of the eddy. Eddies are the principal mechanism for the poleward transport of heat across strong zonal currents. They also transport salt, carbon, and nutrients as they propagate in the ocean and play a significant role in the global budgets of these tracers. Thus, the awareness of the characteristics of eddy and their pathway forms an intrinsic part in understanding ocean dynamics. The wind jets in the equatorial Indian Ocean, between 5° S to 5° N, excite equatorial Kelvin waves which, on reflection from the eastern boundary of the Bay of Bengal, propagate along the perimeter of this basin as a coastal Kelvin wave and radiate Rossby waves (Yu et al. 1991). The coastal Kelvin waves propagate along the perimeter of the Bay of Bengal bend around the Sri Lankan coast and propagate poleward along the west coast of India. The downwelling Kelvin wave radiates downwelling Rossby waves which propagate offshore and promote an anticyclonic circulation in the Laccadive Sea during the winter monsoon. This anticyclonic circulation, called the Laccadive High, develops off the southwest coast of India just north of the Laccadives and at the southern end of the WICC, accompanied by a strong sea surface height anomaly maximum during the late winter monsoon (Bruce et al. 1994; Shankar and Shetye 1997; Bruce et al. 1998). The WICC has to take a large westward detour around the Laccadive High, as observed in the winter monsoon steric height field. They found swirl velocities of about 30 cm s^{-1} and estimated the total transport around the Laccadive High to be about 15 Sv.

As mentioned, the Laccadive High is a mesoscale anticyclonic eddy in the southeastern Arabian Sea formed during the northward phase of the WICC. However, the evolution and role of eddies on coastal currents in the Arabian Sea have not yet been fully understood. The present article attempts to understand how the mesoscale eddies in the ocean can alter the characteristics of the WICC by using in situ measurements and trace its evolution using the satellite-derived sea level anomalies. The material and methods used in the experiment are described in "Material and methods," and the results are presented in "Results." Eddy features, behavior, and its influence on coastal currents are discussed in "Discussions." In the final section, we summarize the main results and briefly describe the conclusions of the work.

Material and methods

As a part of the project entitled "Near shore dynamics of the southwest coast of India with special reference to upwelling and mudbanks," series of current measurements were carried out in the coastal waters of Kerala

by the CSIR-National Institute of Oceanography during 2004–2007. For the present study, current meter records at Kollam (8.94° N, 76.49° E) and Kannur (11.80° N, 75.34° E) on the Indian southwest coast (Fig. 1) for a month during November–December 2005 were used. Currents were measured using current meters (Aanderaa self-recording current meters) on the inner shelf within the 20-m isobaths. The current meters were located at the surface and bottom in the water column: the water column depths at the two current meter locations are given in Table 1. The currents were measured at an interval of 10 min. The current data were first de-tided using the software Tidal Analysis Software Kit (TASK) (Bell et al. 1998). Removal of the tidal component from the current observations leaves residuals that include the contributions from direct and indirect wind forcing, surface waves, and horizontal and vertical density gradients (Prandle 1997). The de-tided (residual) current components (cross-shore and cross-shore) were then rotated to yield the along-shore and cross-shore components.

An earlier study (Aparna et al. 2005) has shown that anemometer winds on the Indian west coast are significantly correlated with the winds measured by the QuikSCAT scatterometer; the QuikSCAT winds are estimated at a standard height of 10 m. Hence, the daily wind speed and direction for the points (8.88° N and 76.38° E; 11.88° N and 75.13° E) close to the study area are used to delineate the role of wind on coastal currents. The alongshore transports in the coastal belt were greatly dependent on the cross-shore component of the wind. Accordingly, the Ekman mass transport derived from the cross-shore wind stress was used at Kollam and Kannur (hereafter station 1 and station 2, respectively). The decomposition was done using the average angle of orientation of the coast in the vicinity of the mooring locations.

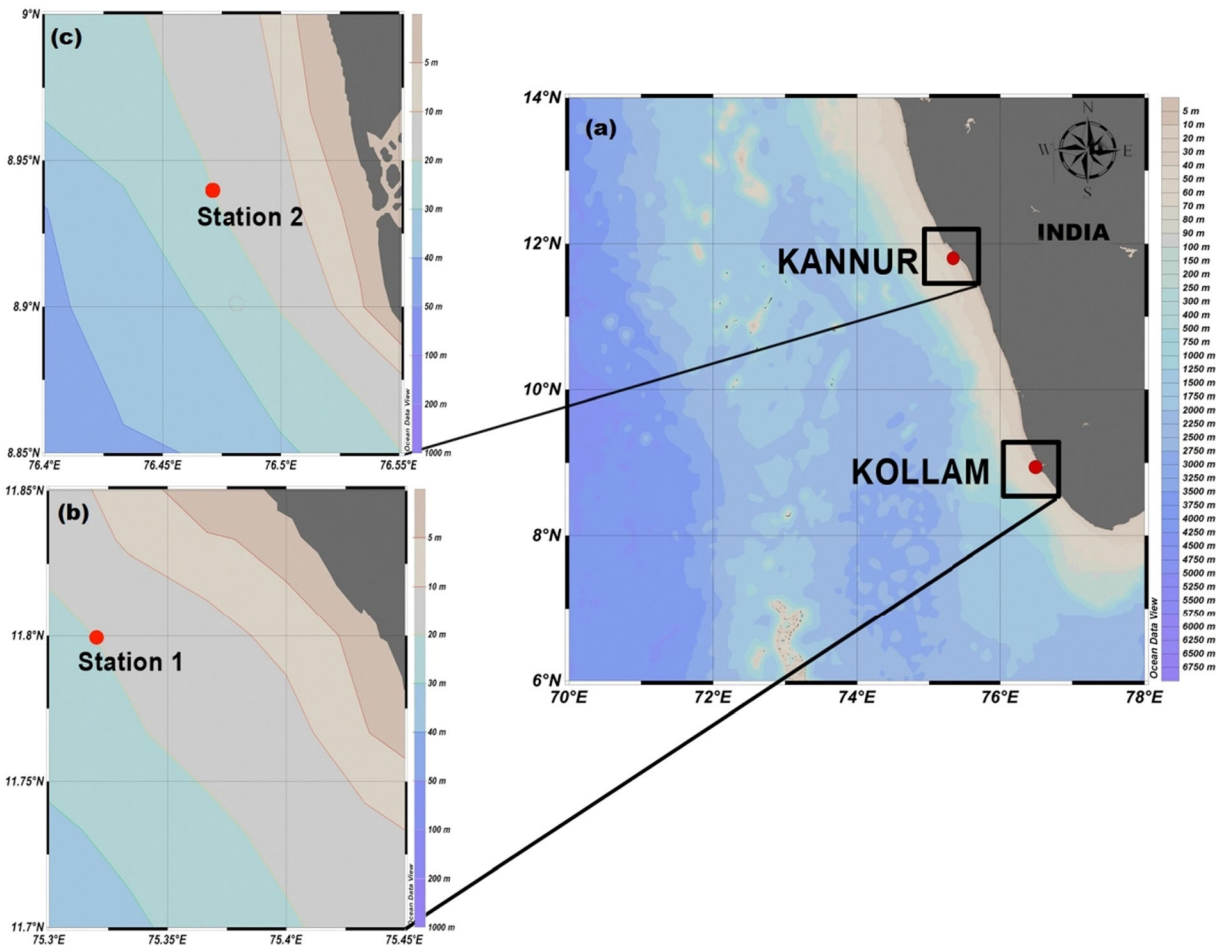

Fig. 1 Location (*red dot*) of the current meter moorings at Kollam (station 1) and Kannur (station 2) in the eastern Arabian Sea (**a**). **b**, **c** Zoom on the stations together with the isobaths

Table 1 Details of the current meter moorings

Sr. no.	Location	Latitude (°N)	Longitude (°E)	Water depth (m)	Level of current meter (m)	Period of measurement	
						From	To
1	Kollam (station 1)	08.94	76.49	20	3.0	25-11-2005	26-12-2005
					18.0	25-11-2005	26-12-2005
2	Kannur (station 2)	11.80	75.34	20	3.0	25-11-2005	26-12-2005
					18.0	25-11-2005	26-12-2005

Over the last decade, satellite altimetry has proved to be a powerful tool to monitor the sea level variability and ocean circulation, leading to the tremendous progress in our knowledge of large to mesoscale ocean dynamics. The inter-comparison analysis of sea level with in situ measurements demonstrated that the altimetry is an important tool to observe oceanic variability even in the coastal regions (Aman et al. 2007; Arnault et al. 1992). Thus, weekly Topex/Poseidon Jason Mission sea surface height (SSH) anomaly data from the National Oceanic and Atmospheric Administration was used to investigate the mesoscale features in the eastern Arabian Sea. To understand the large-scale variability in the coastal region, gridded SSH anomaly maps are used. The cross-shore and along-shore components of surface geostrophic currents were computed from an SSH anomaly. The daily cross-shore and along-shore components of geostrophic currents (downloaded from http://www.aoml.noaa.gov) at the current meter mooring locations were used to scrutinize the influence of geostrophic currents on coastal currents.

Morlet wavelet power spectra are applied for currents (residual and geostrophic) to decompose the assorted modes of variation in the time series. The wavelet transform is a useful alternative to the fast Fourier transform for spectral analysis. It has an advantage of seeing the non-stationary time series in both the time and frequency domains simultaneously. In the wavelet plots, the abscissa is the period in hours and the ordinate in Julian days for residual and geostrophic currents.

Results

Variability of measured currents at the south and northern mooring stations

The currents measured at the surface and bottom at the two mooring stations (station 1 and station 2) during the winter monsoon of 2005 are illustrated. At the southern mooring station (station 1), the mean surface current speed was 13.02 cm s^{-1}, whereas the bottom current speed was 9.58 cm s^{-1}. At the northern mooring station (station 2), the mean current speed at the surface and bottom was 15.15 and 4.2 cm s^{-1}, respectively. The stick plots of current velocity vectors at the surface and bottom for a period of 30 days (Julian days 330–359) are represented in Fig. 2a–d. At station 1, surface currents were initially directed towards north and changed to a southeasterly direction within a short span of 24.00 h (Fig. 2a). The magnitude of current during this period reaches 55–60 cm s^{-1}. Thereafter, the current sustained its direction with less amplitude during the first half of December. Later, there was an abrupt change in the direction of the flow with a maximum velocity of ~60 cm s^{-1} and the current was towards north. Then, the currents deflected from northerly to southerly with increased magnitude (~55 cm s^{-1}). The bottom currents at this station were predominantly southward (Fig. 2c). At station 2, the surface current had a strong northward trend with a maximum velocity of ~50 cm s^{-1}, while a reversal in the current pattern was observed during the last phase of observation (Fig. 2b). The bottom current showed a drastic decrease in speed; nevertheless, the currents were predominantly northward (Fig. 2d). The direction of bottom currents at this station was comparable to that of surface currents.

Temporal variability of cross-shore and along-shore components of currents

The time series of cross-shore and along-shore velocity components of currents at the surface and bottom are presented in Fig. 3a–d. At station 1, the cross-shore currents at the surface and bottom were less intense and had a west to east ($u > 0$) and east to west ($u < 0$) orientation. The maximum velocities at the surface and

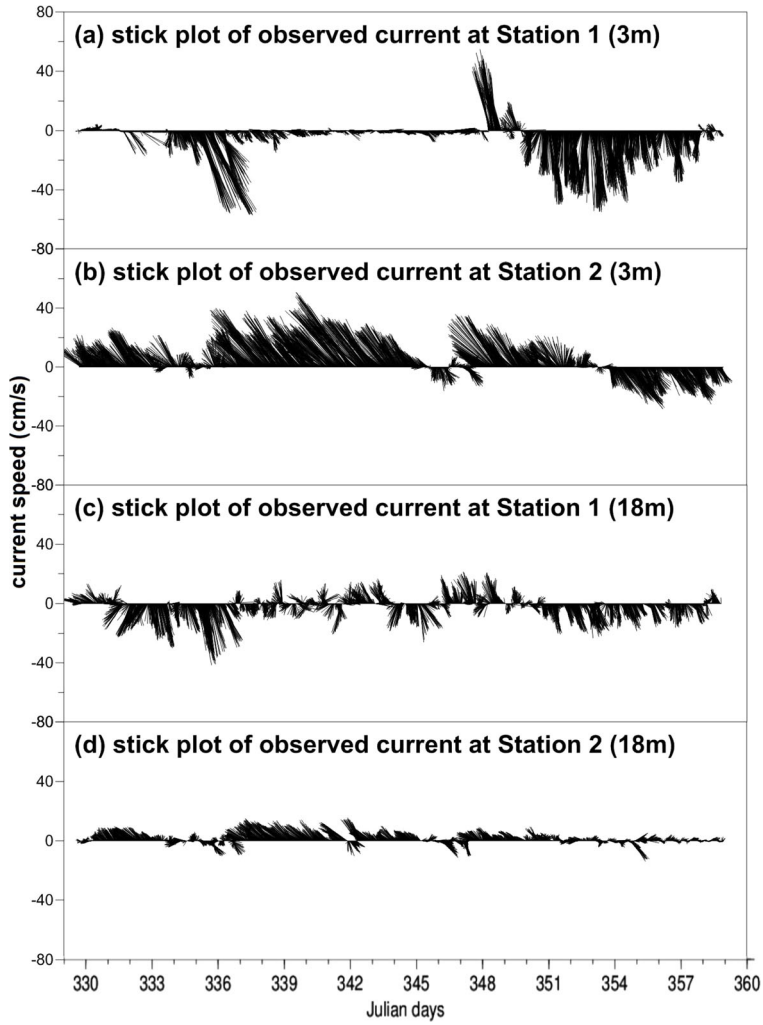

Fig. 2 **a**–**d** Stick plot of the measured current vector during the period of observations

bottom varied from −12.97 to 30.57 cm s^{-1} and −14.69 to 23.78 cm s^{-1}, respectively (Fig. 3a). The mean cross-shore components of currents at the surface and bottom were in opposite direction and suggested a strong stratification of the water column at this station. The along-shore surface current was predominantly southward during the first half of December (Fig. 3a). Shortly, the along-shore velocity component, in turn, had maximum intensities varying between 50 and 55 cm s^{-1} and prevailing southward during the last phase of observation. The cross-shore components of currents at the surface and bottom were negatively correlated whereas the along-shore components of currents at these depths were positively correlated. At station 2, the current velocity of cross-shore components at the surface and bottom showed dominant negative values during the observation period (Fig. 3c, d). Along-shore components of current at these depths were initially directed towards north and changed towards south during the final phase of the observation. The cross-shore and along-shore components of currents at the surface and bottom were positively correlated at this station. The along-shore component of currents was more dominant than the cross-shore component at all the stations. At station 1, the upwelling-favorable (downwelling favorable) along-shore flow is often accompanied by an offshore (onshore) drift, but this is not true at station 2, where a predominant poleward (equator-ward) flow is matched by an onshore (offshore) flow.

Figure 4a–d represents the time series of cross-shore and along-shore components of residual currents at station 1 and station 2. At station 1, cross-shore components of residual currents at the surface and bottom were negatively correlated whereas the along-shore currents were

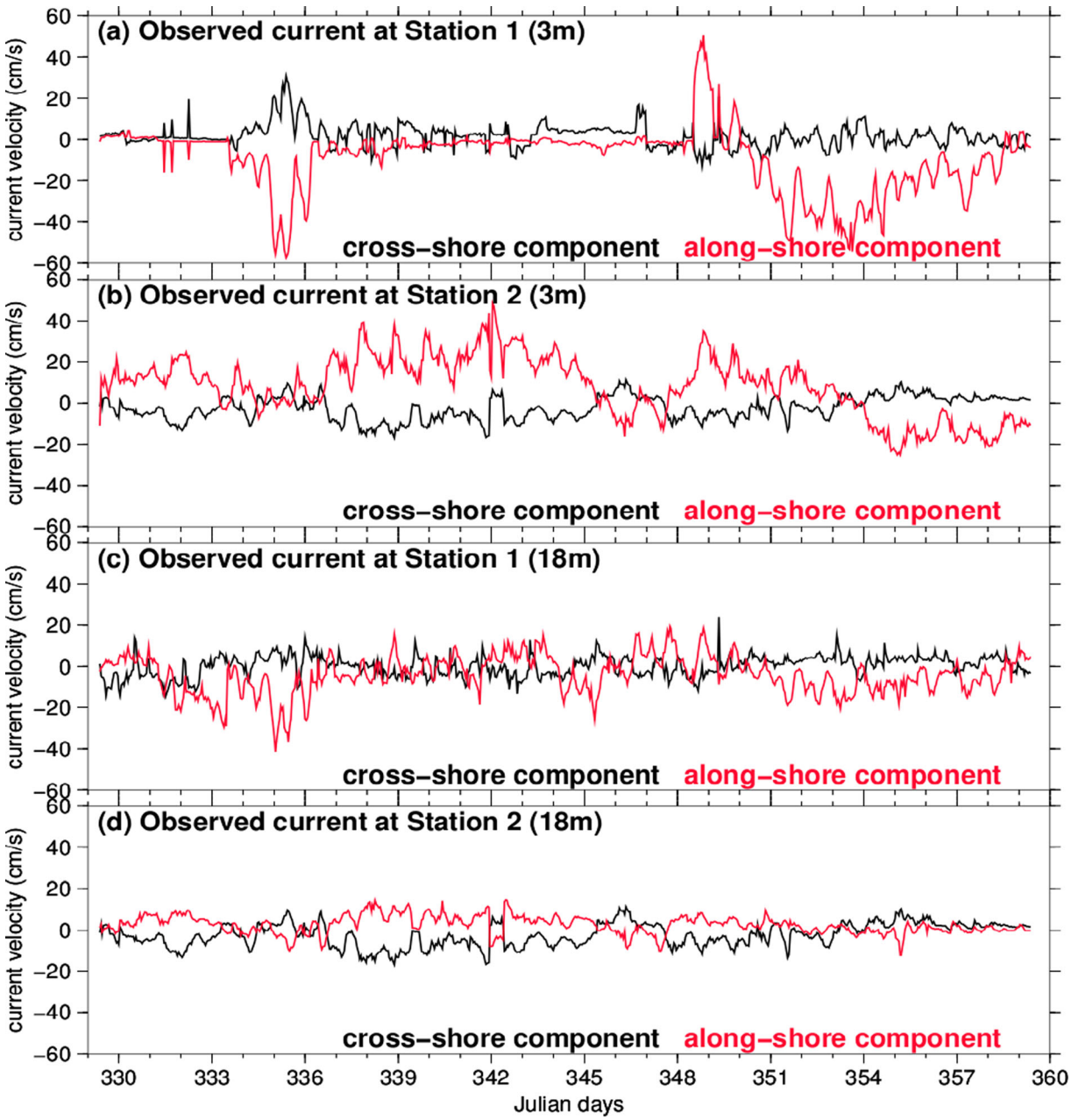

Fig. 3 **a**–**d** Variation of cross-shore and along-shore components of the measured current during the period of observations

positively correlated. The cross-shore and along-shore residual currents at these depths were showing a dominant southeastward current at this station (Fig. 4a). At station 2, correlations between the along-shore component of measured and residual currents at the surface and bottom were 0.73 and 0.82, respectively. The along-shore currents at the surface and bottom were predominantly southward while the pronounced variations in cross-shore components at these depths were absent (Fig. 4c). The along-shore current was high (−30.82 to 30.25 cm s^{-1}) in the near-surface layer and decreased (−16.50 to 11.81 cm s^{-1}) rapidly with depth. However, the variation in cross-shore components of residual currents at the surface (−12.35 to 11.88 cm s^{-1}) and bottom (−9.61 to 10.48 cm s^{-1}) had approximately the same intensities (Fig. 4c, d). The mean cross-shore components of residual currents at all depths were predominantly westward (offshore) at both the stations. The along-

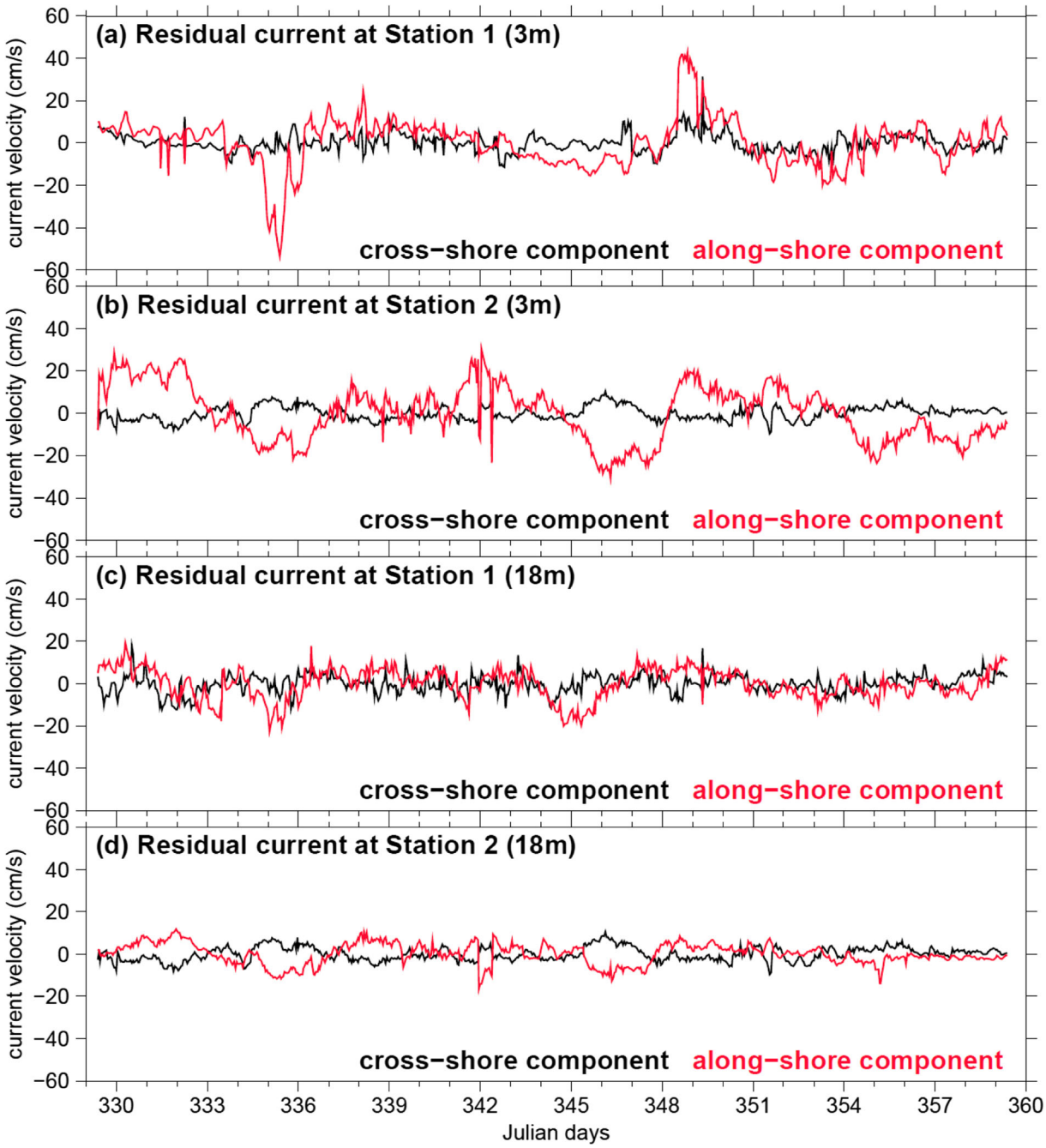

Fig. 4 **a**–**d** Variation of cross-shore and along-shore components of the residual current during the period of observations

shore components of residual currents at the stations were extremely comparable to those of observed currents.

Wind forcing

The wind was predominantly from north to northwesterly with an average speed of 5.75 and 5.08 m s^{-1} at station 1 and station 2, respectively. As the prevailing winds were northerly and northwesterly and with the offshore transport of surface water, the conditions were favorable for upwelling. It is well known that the along-shore current could be generated due to the Ekman transport by the cross-shore wind stress, either an east to west ($u < 0$) or a west to east ($u > 0$) orientation.

Ekman transport derived from the cross-shore wind stress (τ_x) at the stations suggested that a dominant positive (poleward) sign for Ekman transport at station 1 was due to the cross-shore component of easterly wind stress. At station 2, a negative (equator-ward) sign for Ekman transport suggested that the cross-shore component of westerly wind stress was dominant. The cross-shore component of easterly (westerly) wind stress brings poleward (equator-ward) Ekman transport along the west coast of India.

Sea surface height anomaly and geostrophic currents in the eastern Arabian Sea

Sea surface height (SSH) anomaly and geostrophic current data sets describes the evolution of two anticyclonic eddies in the eastern Arabian Sea during the observation period (Fig. 5). A large anticyclonic meander was formed at ~7° N, and the geostrophic current bifurcated northward and southeastward during the initial phase of observation (Fig. 5a). The northward component of the geostrophic current continued a poleward flow along the coast, while the southeastward component created a southward flow at this station. The meander appeared to have evolved into an anticyclonic eddy which strengthened during the final phase of the observation. By 1 December, anticyclonic circulation intensified to become an eddy characterized by a strong positive SSH anomaly (Fig. 5b). Increased spatial extent of the anticyclonic feature over the period of observation was indicative of its intensification although the negative SSH anomaly at the north of the eddy had retained its strength. SSH anomaly for 8 December (Fig. 5c) showed that the anticyclonic eddy had further

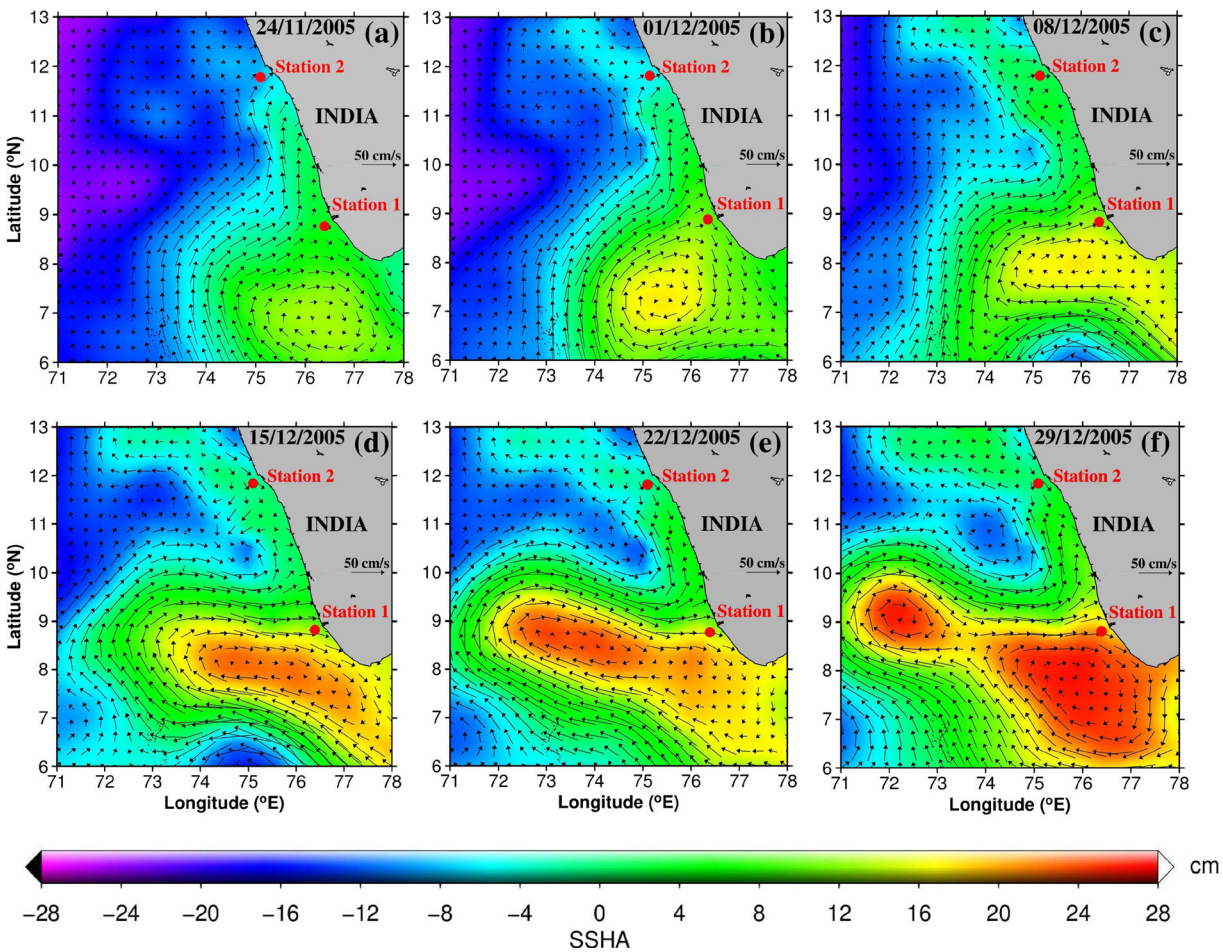

Fig. 5 **a**–**f** Sea surface height anomaly and geostrophic current pattern in the eastern Arabian Sea during the period of observations. Location (*red dot*) of the current meter moorings at station 1 and station 2 in the eastern Arabian Sea

intensified and by 15 December (Fig. 5d), the eddy propagated westward. The deformation of the anticyclonic eddy was noticed resulting in the formation of a secondary eddy, further westward during 22 December (Fig. 5e). By 29 December, this eddy was completely detached from the parent eddy and it sustained its direction with an average speed of ~15 km per day (Fig. 5f). The core of the eddy was located at 9° N and 72° E with a dynamic height anomaly of ~28 cm which was identical to that of the parent eddy. The bifurcated geostrophic current at the northern edge of the eddy further flows poleward associated with a positive SSH anomaly. The poleward flow swirls around an another high in sea level which creates a subsequent anticyclonic eddy centered at 73.50° E and 13° N. The geostrophic current completes the circulation around the eddy, forcing an equator-ward flow along the coast during the last phase of observation.

Discussions

The SSH anomaly and geostrophic current described the anticyclonic eddy evolution in the eastern Arabian Sea during the winter monsoon of 2005. An anticyclonic eddy in the eastern Arabian Sea characterized by a strong positive SSH anomaly was noticed from 1 December. The poleward flow is along the western flank of this anticyclonic eddy, and the geostrophic current completes the circulation around the eddy. The geostrophic current at the northern edge of an anticyclonic eddy is bifurcated into northward and eastward components at ~9° N. The northward component continued a strong poleward flow along the coast with a positive SSH anomaly. The eastward component of the geostrophic current merges with a mean southward flow along the coast at station 1. An intensification of the anticyclonic eddy is noticed during 8 December, which further migrated westward by 15 December. The deformation of an anticyclonic eddy

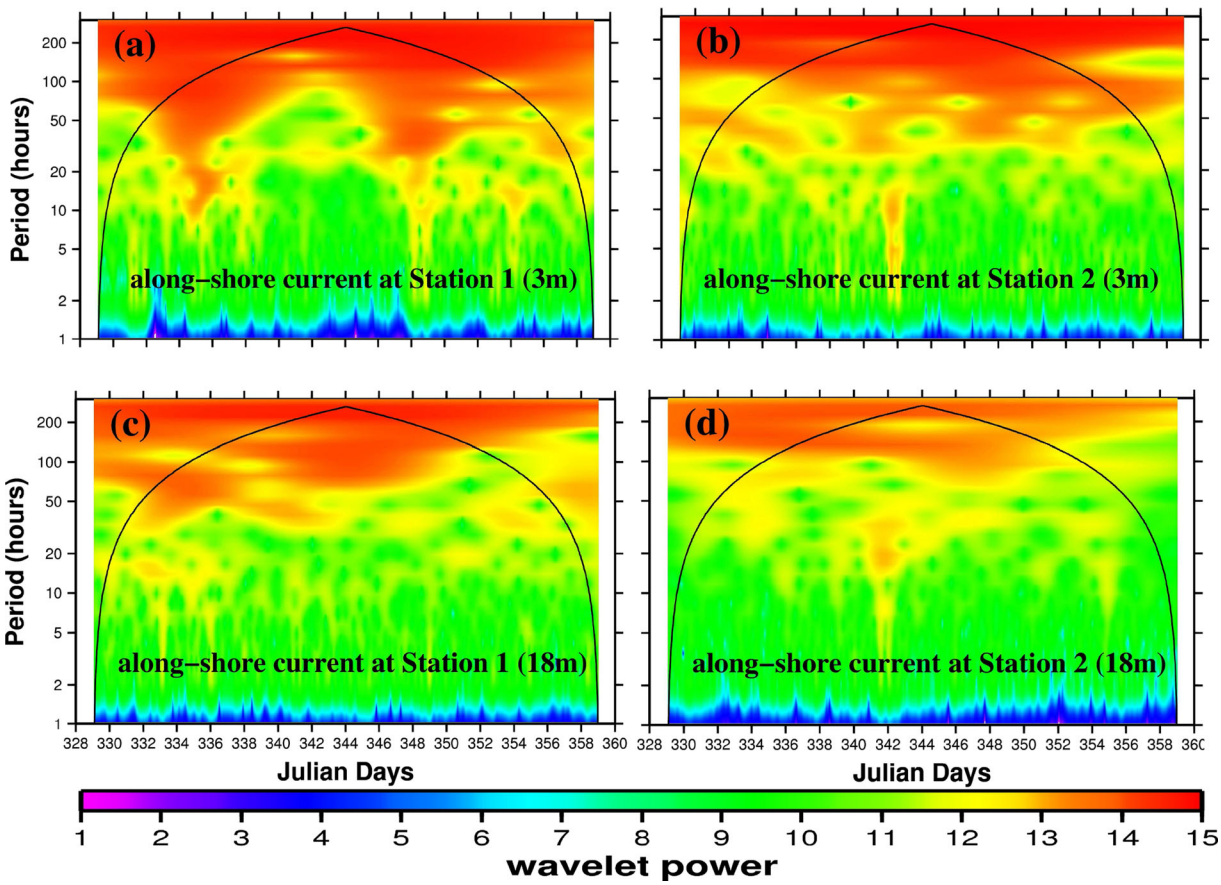

Fig. 6 **a**–**d** Morlet wavelet power spectra for along-shore components of residual currents at station 1 and station 2. The *thick black lines* show the cone of influence (COI) for the wavelet power spectra. The wavelet power is shown in logarithmic scale to the base 2

was noticed from 22 December, which finally splitted into two eddies on 29 December and sustained its direction with an average speed of ~15 km per day. The poleward flow generated by the northward component of the geostrophic current associated with a positive SSH anomaly creates another anticyclonic eddy at 73.5° E and 13° N. The meandering of the geostrophic current around the eddy is observed during this period. The eastward component of the geostrophic current bifurcating from the northern edge of the eddy coalesces with a southward flow along the coast at station 2.

Current measurements at the stations showed a dominant along-shore flow than the cross-shore flow. It is well known that the along-shore current could be generated due to the Ekman transport by the cross-shore wind stress, either an east to west ($u < 0$) or a west to east ($u > 0$) orientation. When the wind is eastward (westward), the positive (negative) sign for surface Ekman transport is taken as poleward (equator-ward) transport and vice versa (Pankajakshan et al. 1997). The currents at the stations were against the prevailing wind induced current clearly depicts the influence of mesoscale process in our study area. Wavelet analysis of along-shore components (residual) of the surface and bottom currents at the stations reveals a band of high-frequency oscillations of 4–8 days' periodicity (Fig. 6). The wavelet analysis of along-shore components of the geostrophic currents at the stations also showed similar fluctuations of 4–8 days' periodicity

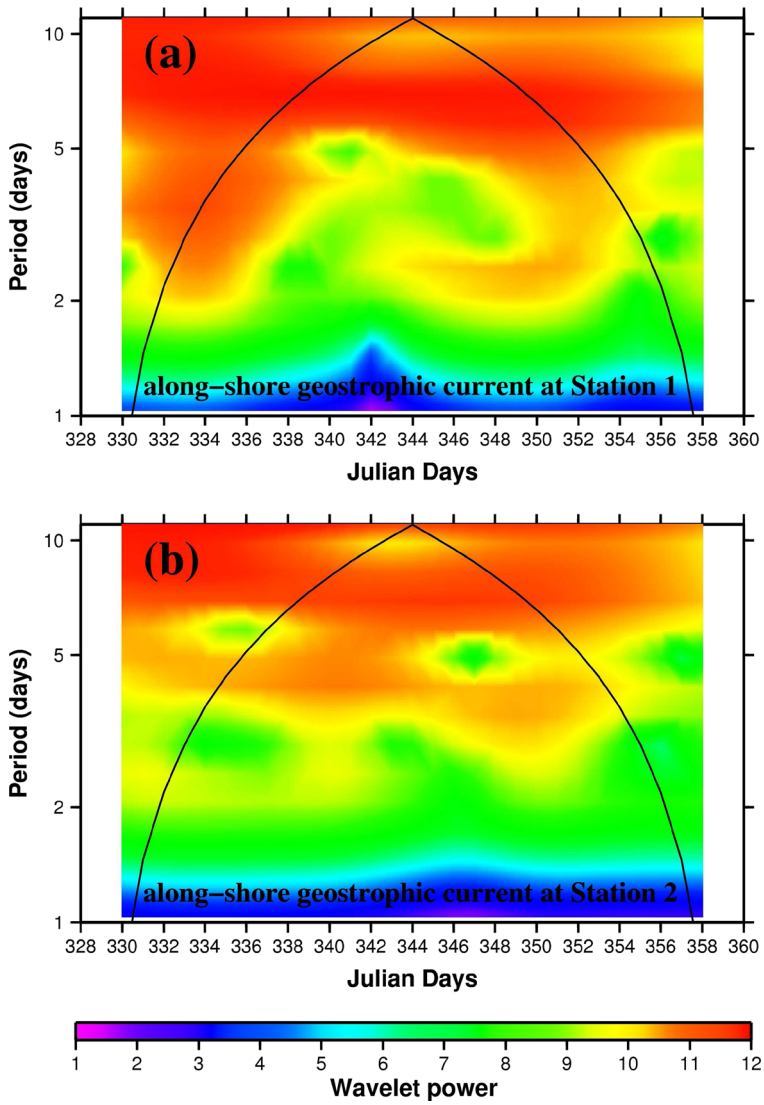

Fig. 7 **a**, **b** Morlet wavelet power spectra for along-shore components of geostrophic currents at station 1 and station 2. The *thick black lines* show the cone of influence (COI) for the wavelet power spectra. The wavelet power is shown in logarithmic scale to the base 2

(Fig. 7). The similar periodicities observed from the wavelet analysis of both residuals and geostrophic currents at the stations suggested that the currents were found to be predominantly in a geostrophic balance.

The general circulation pattern occurring in the study region during eddy formation is summarized in Fig. 8. The two anticyclonic eddies in the eastern Arabian Sea are characterized by a strong poleward flow of the WICC along the western flank, and the geostrophic current completes the circulation around the eddy. The geostrophic current at the northern edge of the eddy is bifurcated into northward and eastward components. The northward component continued as a poleward flow whereas the eastward component merges with a southward flow along the coast. Current measurements at station 1 showed a dominant southward current (60 cm s^{-1}) which weakened with increasing depth (40 cm s^{-1}). The station is located within the perimeter of an anticyclonic eddy, centered at 75° E and 9° N. The eastward component of the geostrophic current bifurcated at the northern edge of the anticyclonic eddy, forcing an equator-ward coastal current at this station. The temporal variations in the observed current pattern at this station suggested the presence of high-frequency fluctuation due to the geostrophic currents around a large-scale anticyclonic (clockwise) eddy in the WICC. Current records at station 2 had a strong northward current during the initial period with a magnitude of about ~50 and ~20 cm s^{-1} at the surface and bottom, respectively. The prevailing northward current observed at this station was due to the anticyclonic eddy induced poleward flow along the coast. A reversal of the current observed at the surface during the last phase of the observation was followed by the formation of a subsequent anticyclonic eddy centered at 73.5° E and 13° N. The eastward component of the geostrophic current bifurcating from the northern edge of this anticyclonic eddy creates a southward flow along the coast during this period. Eddies with horizontal diameters varying from 50 to 150 km have their own pattern of surface currents, which may be sufficiently strong to reverse the direction of the surface currents. The south (station 1) and north (station 2) stations were located at the eastern periphery of the first and second anticyclonic eddies, respectively. The geostrophic current around these anticyclonic eddies would have forcefully reversed the direction of the WICC during the winter monsoon. The comparable periodicities observed between the wavelet analysis of along-shore components of residual and geostrophic currents at the stations substantiated that the currents were found to be predominantly in a geostrophic balance.

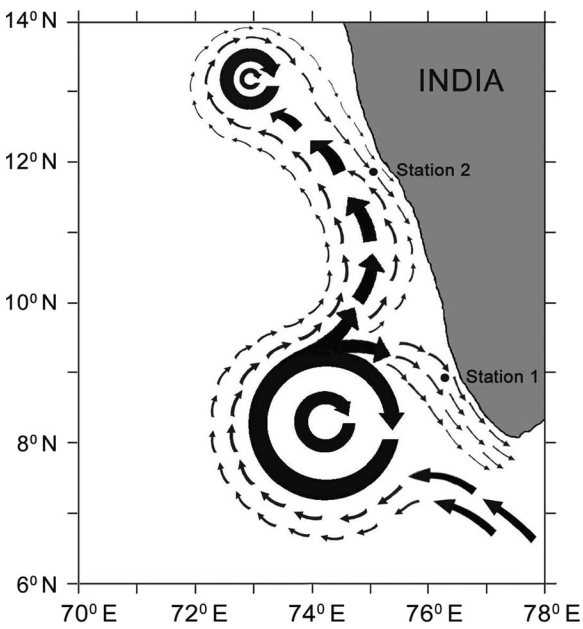

Fig. 8 Schematic representation of the general circulation pattern in the eastern Arabian Sea during the period of observations

Summary and conclusions

The WICC is the seasonally reversing eastern-boundary current of the Arabian Sea which flows equator-ward during the Indian summer monsoon (May–September) and poleward during the winter monsoon (November–February). Measurement of the in situ current velocity field from the study area (station 1 and station 2) contrary to its seasonal cycle was mainly inferred from ship drifts, hydrography, drifters, and satellite altimetry by earlier investigators. Currents in the coastal waters are strongly influenced by winds, tides, propagation of coastal Kelvin and Rossby waves, etc. The present study reveals that the mesoscale features in ocean are also competent to alter the characteristics of coastal currents to a large extent. Analysis of the SSH anomaly and geostrophic currents described the evolution of two anticyclonic eddies in the eastern Arabian Sea during the winter monsoon. Current measurements at the stations showed a forced coastal ocean response to these anticyclonic eddies with the largest response of currents near the surface. An anticyclonic eddy at the southern coast was characterized by a strong positive SSH anomaly, and the geostrophic current

completes the circulation around the eddy. The eastward component of the geostrophic current at the northern edge of the eddy is bifurcated into northward and eastward components. The filaments of the northward component of geostrophic currents get entrained at the eddy perimeter and continue a poleward flow along the coast with a positive SSH anomaly. The eastward component of the geostrophic current eventually merged with the southward-flowing coastal current at ~9° N. The current meter records at station 1 showed the dominant southward current was due to the southward-flowing coastal current at this station. The poleward flow along the coast meanders around another anticyclonic high in sea level at 73.5° E and 13° N during mid December. A dominant northward current at station 2 was associated with this poleward-flowing WICC during the initial period. The eastward component of the geostrophic current at the northern edge of this anticyclonic eddy creates a southward flow which caused a reversal in the current pattern during the last phase of observation. Similar periodicities observed from the wavelet analysis of along-shore components of the residual and geostrophic currents at the stations substantiated that the currents were less influenced by the wind-driven surface current, whereas they were found to be predominantly in a geostrophic balance. The stations were located at the eastern periphery of these two anticyclonic eddies which significantly modifies the characteristics of the WICC during the observation period.

Acknowledgments The authors are thankful to the Director, CSIR-National Institute of Oceanography, and Scientist-in-Charge, CSIR-NIO, Regional Centre, Kochi, for providing facilities for the work. This work is a contribution from the project entitled "Near Shore Dynamics of the southwest coast of India with special reference to Upwelling and Mud banks," which is funded by the Centre for Marine Living Resource and Ecology, Ministry of Earth Sciences, Government of India. Jineesh thanks CSIR for his research fellowship. This work is a part of V.K. Jineesh's doctoral research.

The FORTRAN code for wavelet analysis was downloaded from http://paos.colorado.edu/research/wavelets. This is NIO contribution 5776.

References

Aman, A., Testut, L., Woodworth, P., Aarup, T., & Dixon, D. (2007). Seasonal sea level variability in the Gulf of Guinea from altimetry and tide gauge. *Revue Ivoirienne des Sciences et Technologie*, *9*, 105–118.

Amol, P., Shankar, D., Aparna, S. G., Shenoi, S. S. C., Fernando, V., Shetye, S. R., Mukherjee, A., Agarvadekar, Y., Khalap, S., & Satelkar, N. P. (2012). Observational evidence from direct current measurements for propagation of remotely forced waves on the shelf off the west coast of India. *Journal of Geophysical Research, C: Oceans*, *117*, C05017 15 pp. doi:10.1029/2011JC007606.

Aparna, M., Shetye, S. R., Shankar, D., Shenoi, S. S. C., Mehra, P., & Desai, R. G. P. (2005). Estimating the seaward extent of sea breeze from QuikSCAT scatterometry. *Geophysical Research Letters*, *32*, L13601. doi:10.1029/ 2005GL023107.

Arnault, S., Gourdeau, L., & Menard, Y. (1992). Comparison of the altimetric signal with in-situ measurements in the tropical Atlantic Ocean. *Deep Sea Research Part A: Oceanographic Research Papers*, *39*(3–4), 481–499. doi:10.1016/0198-0149(92)90084-7.

Bell, C., Vassie, J. M., & Woodworth, P. L. (1998). *POL-PSMSL Tidal Analysis Software Kit 2000 (TASK-2000), permanent service for mean sea level*. Merseyside:Proudman Oceanographic Laboratory.

Bruce, J. G., Johnson, D. R., & Kindle, J. C. (1994). Evidence for eddy formation in the eastern Arabian Sea during the northeast monsoon. *Journal of Geophysical Research*, *99*, 7651–7664.

Bruce, J. G., Kipdle, J. C., Kantha, L. H., Kerling, J. L., & Bailey, J. F. (1998). Recent observations and modeling in the Arabian Sea Luccadive high region. *Journal of Geophysical Research*, *103*, 7593–7600. doi:10.1029/97JC03219.

Johannessen, O. M., Subbaraju, G., & Blindheim, J. (1981). Seasonal variations of the oceanographic conditions of the south west coast of India during 1971–1975. *Fiskeridirektoratets Skrifter Serie Havunders*, *18*, 247–261.

McCreary, J. P., Kundu, P. K., & Molinari, R. L. (1993). A numerical investigation of dynamics, thermodynamics and mixed layer processes in the Indian Ocean. *Progress in Oceanography*, *31*, 181–244.

Pankajakshan, T., Patnaik, J., & Ghosh, A. K. (1997). *An atlas of upwelling indices along east and west coast of India*. Goa: Indian National Oceanographic Data Center, National Institute of Oceanography.

Prandle, D., 1997. Tidal and wind driven currents from OSCAR. *Oceanography*, 10(2).

Shankar, D., & Shetye, S. R. (1997). On the dynamics of the Lakshadweep high and low in southeastern Arabian Sea. *Journal of Geophysical Research*, *102*, 12,551–12,562.

Shankar, D., Vinayachandran, P. N., & Unnikrishanan, A. S. (2002). The monsoon currents in the North Indian Ocean. *Progress in Oceanography*, *52*, 63–120.

Shenoi, S. S. C., Shankar, D., & Shetye, S. R. (2004). Remote forcing annihilates barrier layer in southeastern Arabian Sea. *Geophysical Research Letters*, *31*, L05307. doi:10.1029/2003GL019270.

Shetye, S. R. (1998). West India Coastal Current and Lakshadweep high/low. *Sadhana*, *23*(Parts 5 & 6), 637–651.

Shetye, S.R., Gouveia, A.D., 1998. Coastal circulation in the North Indian Ocean—coastal segment (14, S-W). In: Robinson, A. R., Brink, K. H., (eds.), *The Global Coastal Ocean: Regional Studies and Syntheses*. The Sea, 11, 523–556.

Shetye, S. R., Gouveia, A., Shenoi, S. S. C., Michael, G. S., Almeida, A., & Santanam, K. (1990). Hydrography and

circulation of the west coast of India during the southwest monsoon 1987. *Journal of Marine Research*, *48*, 359–378.

Shetye, S. R., Gouveia, A. D., Shenoi, S. S. C., Michael, G. S., Sundar, D., Almeida, A. M., & Santanam, K. (1991). The coastal current off western India during the northeast monsoon. *Deep Sea Research Part I: Oceanographic Research Papers*, *38*, 1517–1529.

Shetye, S. R., Suresh, I., Shankar, D., Sundar, D., Jayakumar, S., Mehra, P., Prabhudesai, R. G., & Pednekar, P. S. (2008). Observational evidence for remote forcing of the West India Coastal Current. *Journal of Geophysical Research*, *113*, C11001.

Stramma, L., Fischer, J., & Schott, F. (1996). The flow field off southwest India at 8° N during the southwest monsoon of August 1993. *Journal of Marine Research*, *54*, 55–72.

Yu, L., O'Brien, J. J., & Yang, J. (1991). On the remote forcing of the circulation in the Bay of Bengal. *Journal of Geophysical Research*, *96*, 20449–20452.